

## Flux-Modulated Andreev Current Caused by Electronic Interference

H. Pothier, S. Guéron, D. Esteve, and M. H. Devoret

*Service de Physique de l'Etat Condensé, Commissariat à l'Energie Atomique, Saclay, F-91191 Gif-sur-Yvette, France*  
(Received 26 April 1994)

We have performed an interference experiment with two tunnel junctions between a thin normal metal wire and a superconducting fork. We have found that the subgap current is strongly modulated by the flux through the resulting normal-superconducting loop. Our results agree with the recent prediction that multiple tunnel attempts of electron pairs, which occur when electrons are confined near the junction, can add coherently if the pair consists of nearly time-reversed states.

PACS numbers: 74.50.+r, 72.10.Fk, 72.15.Rn, 73.40.Gk

Electron tunneling between two normal metal electrodes through an insulating barrier is a basic quantum mechanical phenomenon displaying the wavelike nature of electrons [1]. Interestingly, however, the wave properties of electrons usually manifest themselves in a minimal way: the conductance of such a so-called NN tunnel junction depends only on the area of the barrier, on its transparency, and on the electron densities of both electrodes, as if electrons were classical particles having a certain probability of traversing the barrier each time they collide against it. In particular, the conductance does not depend on the partial confinement of electron wave functions near the barrier [2]. For example, an electron attempting tunneling  $n$  times by zigzagging between impurities in the metal and the tunnel barrier contributes exactly to the conductance, on the average, like  $n$  electrons colliding against the barrier only once. This insensitivity to confinement occurs because the successive tunnel amplitudes in this iterative tunneling do not interfere constructively. On the contrary, constructive interferences in the case of two-electron tunneling at a normal metal-superconductor tunnel junction (NS junction) are robust to phase randomization induced by disorder. Confinement can thus enhance the two-electron conductance, also known as the Andreev conductance [3,4], by a large factor [5]. Consider two nearly conjugated wave functions on the  $N$  side corresponding to nearly time-reversed scattering electron trajectories (Fig. 1). The phase of the two-electron tunnel amplitude at each collision point is the algebraic sum of the phases of the two electrons and of the phase of the superconductor on the other side of the barrier. Therefore, the successive tunneling attempts will add constructively if the phase of the superconductor is constant. If, on the other hand, the iterative tunneling involves two different parts of the barrier with superconducting phases differing by  $\pi$ , destructive interferences will occur [6–8]. We report in this Letter measurements of the two-electron tunnel current as a function of the phase difference imposed between the two halves of a split barrier [7].

We have fabricated “NS-QUIDs” (normal metal-superconductor quantum interference devices) consisting of a normal wire forming two neighboring junctions with

a superconducting fork electrode (see Fig. 2), a design close to one recently proposed by Hekking and Nazarov [8]. The normal wire was made as narrow as possible in order to confine the electrons near the junctions. The difference  $\delta$  between the superconducting phases at the two junctions is controlled by applying a magnetic field perpendicular to the plane of the fork:  $\delta = 2\pi\Phi/\Phi_0$ , where  $\Phi$  is the magnetic flux threading the loop formed by the fork and the wire and  $\Phi_0 = h/2e$ .

Our samples were fabricated using electron beam lithography and shadow-mask evaporation [9]. A 20 nm thick aluminum film was deposited using electron beam evaporation, then oxidized in a 0.15 Torr  $O_2$  (10%) Ar (90%) mixture for 3 minutes. The 30 nm thick copper counter-electrode was then deposited. The samples were mounted in a copper box which was thermally anchored to the mixing chamber of a dilution refrigerator. Current-voltage ( $I$ - $V$ ) measurements were performed using properly filtered coaxial lines [10]. We concentrate here on the results obtained on the sample whose  $I$ - $V$  characteristic was most strongly flux-dependent. From the large scale normal state  $I$ - $V$  characteristic (dashed line in the top-left inset of Fig. 3), measured by applying a field of 0.1 T perpendicular to the films, we obtain  $G_T = 641 \mu S$ . The large

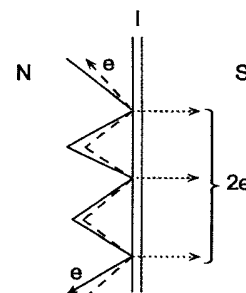


FIG. 1. Semiclassical representation of the mechanism responsible for constructive interferences in iterative tunneling of electron pairs. Two confined electrons in the normal electrode, with nearly time-reversed wave functions, tunnel together through the barrier at different points with the same total phase. If the order parameter of the superconductor is uniform, the tunnel amplitudes at these different points contribute constructively to the total current.

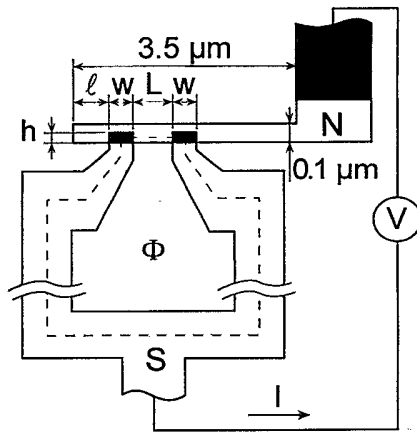


FIG. 2. NS-QUID layout: a normal metal wire overlaps an oxidized superconducting fork electrode to form a split tunnel junction. The effective area of the loop (enclosed by the dotted line) is  $13 \mu\text{m}^2$ . The superconducting bottom electrode (aluminum) and the normal top electrode (copper) were 20 and 30 nm thick, respectively. Regions where the normal electrode overlaps the superconducting electrode are dark. The parameters of the sample whose data are shown in Figs. 3 and 4 were  $w = 230 \text{ nm}$ ,  $h = l = 100 \text{ nm}$ , and  $L = 60 \text{ nm}$ . For clarity, we have not represented the normal metal replica of the loop shifted down by 260 nm.

scale  $I$ - $V$  characteristic at zero field is shown in the same inset as a solid line. As the temperature is decreased below 300 mK, the subgap current becomes strongly field modulated, as shown in the bottom right inset of Fig. 3 for  $V = 20 \mu\text{V}$  and  $T = 27 \text{ mK}$ . The magnetic field dependence of the current follows a sine function (solid line). Assuming a  $\Phi_0$ -periodicity for the modulation as a func-

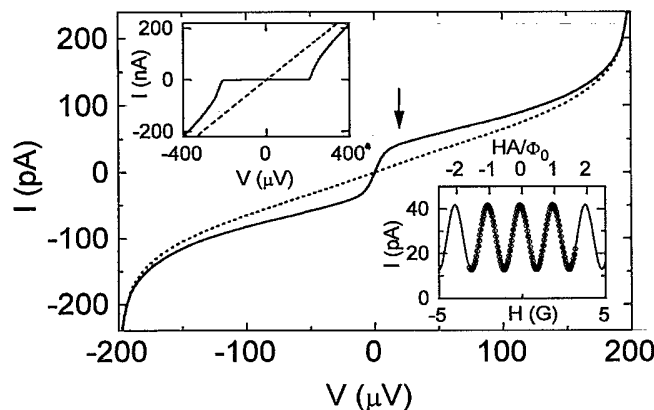


FIG. 3. Extremal subgap  $I$ - $V$  characteristic measured at  $T = 27 \text{ mK}$ . The solid and the dotted lines correspond to maxima ( $\Phi = k\Phi_0$ ) and minima [ $\Phi = (k + 1/2)\Phi_0$ ] of the modulation of the current with the magnetic field  $H$  shown in the bottom-right inset, respectively. The arrow indicates the bias voltage at which the modulation pattern was measured (circles: data; solid line: sine function fit). The top-left inset represents the large scale characteristics of the NS-QUID at  $H = 0$  (solid line) and  $H = 0.1 \text{ T}$  (dashed line).

tion of the flux threading the loop, we deduce an effective field capturing area  $A$  of the loop which agrees within 20% with the area defined in Fig. 2. Note that the positions of the maxima with respect to the external field  $H$  do not correspond exactly with integer multiples of  $\Phi_0$ , an offset which we attribute to the residual field in the cryostat. We show in the main plot of Fig. 3 the two extremal  $I$ - $V$  characteristics (solid and dashed lines). At  $\Phi = k\Phi_0$ , the conductance exhibits a peak at zero voltage, as observed in several experiments [11–13]. The maximal ( $\Phi = k\Phi_0$ ) and minimal [ $\Phi = (k + 1/2)\Phi_0$ ] conductances at  $V = 0$  are  $G_{\text{max}} = 4.6 \mu\text{S}$  and  $G_{\text{min}} = 0.66 \mu\text{S}$ , which are much larger than the ballistic value [14]  $G_{\text{bal}} = (h/4e^2)G_T^2/N_{\text{eff}} \approx 25 \text{ nS}$ , where  $N_{\text{eff}} = S/4\pi\lambda^2$  is the effective number of channels calculated with the upper bound estimate  $\lambda = 0.2 \text{ nm}$  for the barrier wavelength cutoff [15]. Such a large discrepancy with the ballistic model was already pointed out in Refs. [16] and [17]. The flux dependence of the conductance indicates that this discrepancy originates from phase-coherent processes in the normal electrode and not, for example, from leaks in the tunnel barrier.

Figure 4 shows the variations of the peak-to-peak amplitude  $I_{\text{mod}}$  of the current modulation, such as the one shown in the bottom-right inset of Fig. 3, as a function of the bias voltage  $V$ , at temperatures ranging from 27 to 233 mK. The data show that the zero-voltage conductance decreases with temperature, whereas, up to

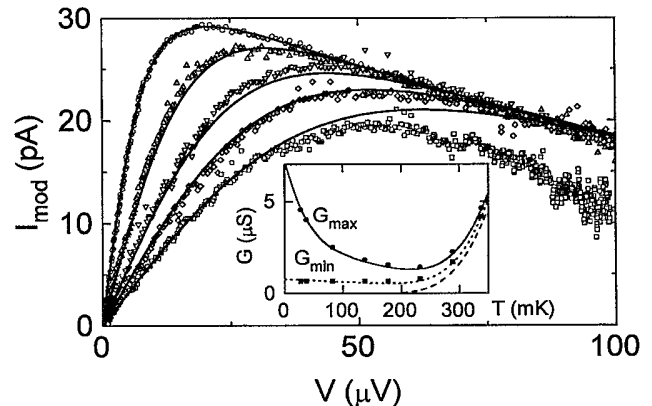


FIG. 4. Comparison between the measured (open symbols) and predicted (solid lines) bias voltage dependence of the peak to peak modulation  $I_{\text{mod}}$  of the current with the magnetic field at different temperatures (top to bottom:  $T = 27, 82, 137, 177,$  and  $233 \text{ mK}$ ). The experimental data were obtained by numerical subtraction of the extremal  $I$ - $V$ s; predicted curves are calculated using formulas (4) and (6), with  $D = 59 \times 10^{-4} \text{ m}^2\text{s}^{-1}$  and  $\tau_\Phi = 120 \text{ ps}$ . We used  $\Delta = 205 \mu\text{eV}$  for the gap in aluminum and  $\nu = 1.5 \times 10^{47} \text{ J}^{-1} \text{ m}^{-3}$  for the density of states of copper. Inset: comparison between the measured (symbols) and predicted (lines) temperature dependences of the maximal and minimal zero-voltage conductances  $G_{\text{max}}$  and  $G_{\text{min}}$ . The dashed line shows the quasiparticle conductance contribution  $G_{\text{qp}}$  to  $G$ .

180 mK, the current becomes temperature independent at voltages of the order of 0.1 mV. In the following, we show that the precise voltage and temperature dependence of  $I_{\text{mod}}$  is qualitatively understood.

The influence of disorder in the normal electrode on the conductance of NS junctions has been treated by several authors [5,14,18]. More recently, Hekking and Nazarov have established the link between the Andreev current and the dynamics of the electrons in the normal electrode and derived an expression for the  $I$ - $V$  characteristic at  $eV \ll \Delta - k_B T$ , where  $\Delta$  is the gap of the superconductor [8,15]. We find that their expression (4) in Ref. [8] can be recast in the form [19]

$$I = \frac{1}{\nu e^2} \int_0^\infty dt K(t) e^{-t/\tau_\Phi} \frac{\pi k_B T \sin(2eVt/\hbar)}{e \sinh(2\pi k_B T t/\hbar)} \quad (1)$$

with the kernel  $K(t)$  given by

$$K(t) = \iint_{(\text{barrier})^2} d^2 r d^2 r' g(r) g(r') e^{i[\varphi(r) - \varphi(r')]} p(r, r', t), \quad (2)$$

where  $p(r, r', t) d^3 r'$  coincides for  $t \gg \hbar/E_F$  with the conditional probability density that an electron in the normal metal prepared at time  $t = 0$  at point  $r$  on the barrier is found at time  $t$  in a volume  $d^3 r'$  around point  $r'$ . The symbol  $g(r)$  denotes the conductance per unit area of the tunnel barrier at point  $r$ . The phase  $\varphi(r)$  of the superconductor is taken at the point across the barrier from point  $r$ . The parameters  $\tau_\Phi$  and  $\nu$  denote the phase-breaking time and the density of states per unit volume at the Fermi energy, including both spin directions, respectively. The phenomenological factor  $e^{-t/\tau_\Phi}$  was added to the original expression of Hekking and Nazarov in order to account for the loss of coherence due to phase-breaking processes. For an NS-QUID, the phase difference  $\varphi(r) - \varphi(r')$  vanishes if  $r$  and  $r'$  are on the same junction and takes the value  $\pm 2\pi\Phi/\Phi_0$  otherwise (for the low fields considered here, the phase along each junction can be taken constant). Therefore,

$$K(t) = K_{11}(t) + K_{22}(t) + 2K_{12}(t) \cos(2\pi\Phi/\Phi_0), \quad (3)$$

where  $K_{ij}(t)$  characterizes electrons going from junction  $i$  to junction  $j$ . Expression (1) thus predicts a sine-modulated component for the NS-QUID current, which we observe in our experiment (see bottom right inset of Fig. 3). We have focused here on the amplitude  $I_{\text{mod}}$  of the current modulation rather than its absolute value since the cross-kernel  $K_{12}(t)$  is more amenable to quantitative calculations than  $K_{11}(t)$  and  $K_{22}(t)$  [ $K_{12}(t)$  is nonzero only for times greater than the electron transit time from one junction to the other]. We have calculated  $K_{12}(t)$  assum-

ing that  $p(r, r', t)$  obeys a diffusion equation with diffusion constant  $D$  inside a flat slab-shaped normal electrode, taking into account the bending of the normal wire over the superconductor through an effective junction width  $w_{\text{eff}} = w + 2d$ . By inserting the result into (1), we find

$$I_{\text{mod}} = \frac{4(h/e^2)G_T^2}{\pi^2 d S e \nu} \int_0^\infty du f(u) h(u), \quad (4)$$

where

$$f(u) = \left[ \frac{\sin(u/2)}{u} \right]^2 \cos\left(\frac{x_1 u}{w_{\text{eff}}}\right) \cos\left(\frac{x_2 u}{w_{\text{eff}}}\right)$$

and

$$h(u) = \text{Im} \Psi \left\{ \frac{1}{2} + \frac{T_0}{T} \left[ 1 + \eta \left( u^2 + i \frac{V}{V_0} \right) \right] \right\},$$

with  $x_1 = l + w_{\text{eff}}/2$ ,  $x_2 = l + L + 3w_{\text{eff}}/2$ ,  $T_0 = \hbar/4\pi k_B \tau_\Phi$ ,  $V_0 = \hbar D/2e w_{\text{eff}}^2$ , and  $\eta = D\tau_\Phi/w_{\text{eff}}^2$ . At zero temperature, it is possible to improve (1) by taking into account the finite  $eV/\Delta$  ratio, and one obtains

$$I = \frac{1}{\nu e^2} \int_0^\infty dt K(t) e^{-t/\tau_\Phi} \int_0^V d\nu \frac{\cos(2e\nu t/\hbar)}{1 - (e\nu/\Delta)^2}, \quad (5)$$

which differs from (1) only near the gap. We can apply this equation to get  $I_{\text{mod}}(\Delta, T = 0)$  and evaluate  $I_{\text{mod}}(\Delta, T)$ , at temperature such that  $k_B T \ll \Delta$ , from

$$I_{\text{mod}}(\Delta, T) \approx I_{\text{mod}}(\Delta = \infty, T) \frac{I_{\text{mod}}(\Delta, T = 0)}{I_{\text{mod}}(\Delta = \infty, T = 0)}, \quad (6)$$

which gives a 5% correction to expression (4) at  $V = 0.1$  mV. In Fig. 4, we compare the predictions of formula (4) corrected by (6) (solid lines) with the data, using  $\nu = 1.5 \times 10^{47} \text{ J}^{-1} \text{ m}^{-3}$ . The fit parameters are  $D = (60 \pm 5) 10^{-4} \text{ m}^2 \text{ s}^{-1}$  and  $\tau_\Phi = 120 \pm 10$  ps, which are compatible with previous measurements [20]. However, we had to scale the calculated  $I_{\text{mod}}$  up by a factor 4.7, which is not understood at present. Allowing for this adjustment, we find a quantitative agreement between experiment and theory at temperatures between 27 mK (top curve) and 180 mK (fourth curve from the top). Only at 230 mK is the modulation smaller than predicted for voltages above 50  $\mu\text{V}$ . This is possibly due to the failure of the approximation (6) at high temperatures.

An expression similar to (4) gives the nonmodulated contribution to the current, which corresponds to the functions  $K_{11}(t)$  and  $K_{22}(t)$ . Scaled with the same factor 4.7, the amplitude of the nonmodulated current fits the measurements at low voltages (comparison not shown), but underestimates the current at voltages above 20  $\mu\text{V}$ . We estimate that the expected extra contribution to the current arising from phase-coherent diffusion of quasipar-

ticles in the superconducting electrode [15,21] is, however, too small to resolve the discrepancy, and we rather believe that the diffusion model itself does not adequately describe the spread-out of electrons at short times. In the inset of Fig. 4, we compare the temperature dependence of the maximal ( $\Phi = k\Phi_0$ ) and minimal [ $\Phi = (k + 1/2)\Phi_0$ ] zero-voltage conductances  $G_{\max}$  and  $G_{\min}$  with theory, also scaled up by the factor 4.7. Above 200 mK, the contribution  $G_{\text{qp}}$  of thermally activated quasiparticle tunneling to the conductance (dashed line) is no longer negligible, and we have added it to the Andreev conductance. The calculated conductances agree with experimental data over the whole temperature range.

We have performed the same analysis on two other samples. The values of the fit parameters were  $D = 53 \times 10^{-4} \text{ m}^2 \text{ s}^{-1}$  and  $\tau_{\Phi} = 25 \text{ ps}$  for the first one and  $D = 133 \times 10^{-4} \text{ m}^2 \text{ s}^{-1}$  and  $\tau_{\Phi} = 16 \text{ ps}$  for the second one. This dispersion might be explained by the fact that the samples were evaporated separately and had different impurity contents. The scaling factors were 2.5 and 3.0, respectively. For these samples, the amplitude of the nonmodulated current was underestimated by theory already near zero voltage.

An alternative interpretation of the data would be to consider that a small superconducting gap develops in the normal metal side of the junctions, because of the proximity effect, and that our NS-QUID can be considered as a SQUID with one superconductor having a small superconducting gap. The current in such a SQUID is indeed expected to have the same flux dependence as in our experiments. However, even with unrealistic parameters, the best fit obtained using the relevant theory [22,23] is very poor.

In conclusion, we have observed that the Andreev conductance of NS-QUIDS in which the normal electrode confines the electrons near the junctions is much larger than predicted by the ballistic model and is strongly modulated by the flux. The model of constructive interferences in iterative Andreev tunneling provides a quantitative explanation of the voltage and temperatures dependence of the flux-modulated current.

We have benefited from many discussions with F. Hekking and Yu. Nazarov. We are grateful to T. M. Klapwijk for useful comments on our results and to G.-L. Ingold for help in the preparation of the manuscript.

[1] L. Solymar, *Superconductive Tunnelling and Applications* (Chapman and Hall, London, 1972), Chap. 1.

- [2] Fluctuations of the differential conductance as a function of the bias voltage could, however, be influenced by confinement: see Yu. Nazarov, *Zh. Eksp. Teor. Fiz.* **98**, 306 (1990) [*Sov. Phys. JETP* **71**, 171 (1990)].
- [3] A. F. Andreev, *Zh. Eksp. Teor. Fiz.* **46**, 1823 (1964) [*Sov. Phys. JETP* **19**, 1228 (1964)].
- [4] G. E. Blonder, M. Tinkham, and T. M. Klapwijk, *Phys. Rev. B* **25**, 4515 (1982).
- [5] B. J. van Wees, P. de Vries, P. Magnée, and T. M. Klapwijk, *Phys. Rev. Lett.* **69**, 510 (1992).
- [6] Different effects involving the phase difference between two superconductors have already been considered in B. Z. Spivak and D. E. Khmel'nitskii, *Pis'ma Zh. Eksp. Teor. Fiz.* **35**, 334 (1982) [*JETP Lett.* **35**, 412 (1982)] and in B. L. Al'tshuler and B. L. Spivak, *Zh. Eksp. Teor. Fiz.* **92**, 609 (1987) [*Sov. Phys. JETP* **65**, 343 (1987)].
- [7] H. Nakano and H. Takayanagi, *Solid State Commun.* **80**, 997 (1991).
- [8] F. W. Hekking and Yu. Nazarov, *Phys. Rev. Lett.* **71**, 1625 (1993).
- [9] G. J. Dolan and J. H. Dunsmuir, *Physica (Amsterdam)* **152B**, 7 (1988).
- [10] J. M. Martinis, M. H. Devoret, and J. Clarke, *Phys. Rev. B* **35**, 4682 (1987).
- [11] A. Kastalsky, L. H. Greene, J. B. Barner, and R. Bhat, *Phys. Rev. Lett.* **64**, 958 (1990); A. W. Kleinsasser, T. N. Jackson, D. McInturff, F. Rammo, G. D. Petit, and J. M. Woodall, *Appl. Phys. Lett.* **57**, 1811 (1990); A. Kastalsky, A. W. Kleinsasser, L. H. Greene, R. Bhat, F. P. Milliken, and J. P. Harbison, *Phys. Rev. Lett.* **67**, 3026 (1991).
- [12] C. Nguyen, H. Kroemer, and E. L. Hu, *Phys. Rev. Lett.* **69**, 2847 (1992).
- [13] P. Xiong, G. Xiao, and R. B. Laibowitz, *Phys. Rev. Lett.* **71**, 1907 (1993).
- [14] C. W. J. Beenakker, *Phys. Rev. B* **46**, 12 841 (1992).
- [15] F. W. Hekking and Yu. Nazarov, *Phys. Rev. B* **49**, 6847 (1994).
- [16] T. M. Eiles, J. M. Martinis, and M. H. Devoret, *Phys. Rev. Lett.* **70**, 1862 (1993).
- [17] J. M. Hergenrother, M. T. Tuominen, and M. Tinkham, *Phys. Rev. Lett.* **72**, 1742 (1994).
- [18] A. F. Volkov, A. V. Zaitsev, and T. M. Klapwijk, *Physica (Amsterdam)* **210C**, 21 (1993).
- [19] We have corrected a factor  $1/4\pi^2$  missing in Ref. [8] [Yu. Nazarov (private communication)].
- [20] B. Pannetier, J. Chaussy, and R. Rammal, *Physica Scripta* **T13**, 245 (1986).
- [21] D. V. Averin and Yu. Nazarov, *Phys. Rev. Lett.* **69**, 1993 (1992).
- [22] A. Barone and G. Paternò, *Physics and Applications of the Josephson Effect* (Wiley-Interscience, New York, 1982).
- [23] G.-L. Ingold, H. Grabert, and U. Eberhardt, *Phys. Rev. B* **50**, 395 (1994).